

Thermodynamics of the two-dimensional frustrated J_1 - J_2 Heisenberg ferromagnet in the collinear stripe regime: Susceptibility and correlation length

M. Härtel, J. Richter, and O. Götze

Institut für Theoretische Physik, Otto-von-Guericke-Universität Magdeburg, D-39016 Magdeburg, Germany

D. Ihle

Institut für Theoretische Physik, Universität Leipzig, D-04109 Leipzig, Germany

S.-L. Drechsler

Leibniz-Institut für Festkörper- und Werkstoffforschung Dresden, D-01171 Dresden, Germany

(Dated: November 9, 2018)

We calculate the temperature dependence of the correlation length ξ and the uniform susceptibility χ_0 of the frustrated J_1 - J_2 square-lattice Heisenberg ferromagnet in the collinear stripe phase using Green-function technique. The height χ_{max} and the position $T(\chi_{max})$ of the maximum in the $\chi_0(T)$ curve exhibit a characteristic dependence on the frustration parameter $J_2/|J_1|$, which is well described, for $J_2 > 0.7|J_1|$, by the relations $\chi_{max} = a(J_2 - J_2^c)^{-\nu}$ and $T(\chi_{max}) = b(J_2 - J_2^c)$, where $J_2^c = 0.4|J_1|$ and ν is of the order of unity. The correlation length diverges at low temperatures as $\xi \propto e^{A/T}$, where A increases with growing $J_2/|J_1|$. We also compare our results with recent measurements on layered oxovanadates and find reasonable agreement.

PACS numbers:

I. INTRODUCTION

Frustrated square-lattice quantum magnets have been in the focus of active condensed-matter investigations in recent years. While for the study of ground state (GS) properties many alternative methods, such as exact diagonalization (ED),¹⁻⁴ the Schwinger boson approach,⁵ functional renormalization group method,⁶ the tensor-product approach,⁷ or the coupled-cluster method (CCM)⁴ can be applied, there are much less reasonable theoretical approaches available to deal with thermodynamic properties of these systems. On the other hand, there are many recent experimental studies on quasi-two-dimensional frustrated square-lattice compounds, see, e.g., Refs. 8–17, where typically temperature dependent properties are reported, which should be compared with theoretical predictions. The quantum Monte Carlo technique is not applicable due to the sign problem for frustrated systems.¹⁸ The high-temperature expansion approach^{19,20} is limited to temperatures down to the order of the exchange coupling. Full ED studies used in Refs. 21–23 for the J_1 - J_2 square-lattice Heisenberg ferromagnet of $N = 8, 16$ and 20 sites suffer from finite-size effects at lower temperatures.^{20,24} An alternative method to describe quantum magnets in the whole temperature range is the Green-function technique.²⁵⁻²⁷ A rotationally invariant second-order Green-function theory has been applied successfully to describe the thermodynamics of frustrated quantum magnets.^{24,28-32} In particular, the Green-function technique is designed for $N \rightarrow \infty$ and allows the calculation of the magnetic correlation length, in addition to the usual thermodynamic quantities, such as the susceptibility.

Motivated by recent measurements of the correlation lengths for several frustrated layered Heisenberg square-

lattice ferromagnets,¹⁵ in the present paper we study the temperature dependence of the correlation length and the uniform susceptibility of the spin-1/2 J_1 - J_2 model

$$H = J_1 \sum_{\langle i,j \rangle} \mathbf{S}_i \mathbf{S}_j + J_2 \sum_{\langle\langle i,j \rangle\rangle} \mathbf{S}_i \mathbf{S}_j, \quad (1)$$

where $\langle \dots \rangle$ denotes the nearest neighbor (NN) and $\langle\langle \dots \rangle\rangle$ the next-nearest neighbor (NNN) bonds on a square lattice. We consider a ferromagnetic NN coupling $J_1 < 0$ and a frustrating antiferromagnetic NNN coupling $J_2 > 0$. The GS of this model has been discussed in Refs. 2,4,5. At $J_2 = J_2^c \approx 0.4|J_1|$ the ferromagnetic GS present at small J_2 gives way for a GS phase with zero total magnetization. Although, the nature of this state for $J_2 \gtrsim J_2^c$ is still under debate, the existence of antiferromagnetic collinear stripe GS long-range order (LRO) for $J_2 > 0.7|J_1|$ is not questioned.

Following our previous investigation of this model, see Ref. 24, we use the rotationally invariant second-order Green-function method (RGM) to calculate the thermodynamic properties. However, by contrast to Ref. 24, where the model was studied in the ferromagnetic regime, i.e. $J_2 < J_2^c$, here we focus on the antiferromagnetic collinear stripe GS regime. We restrict our study on the parameter region $J_2 > 0.7|J_1|$, that corresponds to the experimental situation for several layered oxovanadates.^{8,9,15}

The paper is organized as follows. In Sec. II the RGM applied to the J_1 - J_2 square lattice is illustrated. The results for the susceptibility and correlation length and the comparison to recent experimental data is presented in Sec. III. Finally, a short summary is given in Sec. IV.

II. ROTATIONALLY INVARIANT GREEN-FUNCTION METHOD (RGM)

The RGM was introduced by Kondo and Yamaji.³³ The method was further developed and applied to Heisenberg magnets by several groups, see, e.g., Refs. 24,28–32,34–43.

To calculate the dynamical transverse spin susceptibility $\chi_q^{+-}(\omega)$ we have to determine the two-time commutator Green function $\langle\langle S_q^+; S_{-q}^- \rangle\rangle_\omega = -\chi_q^{+-}(\omega)$. The equation of motion for $\langle\langle S_q^+; S_{-q}^- \rangle\rangle_\omega$ up to second order reads $\omega^2 \langle\langle S_q^+; S_{-q}^- \rangle\rangle_\omega = M_q + \langle\langle -\ddot{S}_q^+; S_{-q}^- \rangle\rangle_\omega$ with $-\ddot{S}_q^+ = [[S_q^+, H], H]$ and the exact moment

$$M_q = -8J_1 C_{1,0} \left(1 - \gamma_q^{(1)}\right) - 8J_2 C_{1,1} \left(1 - \gamma_q^{(2)}\right), \quad (2)$$

where $\gamma_q^{(1)} = (\cos q_x + \cos q_y)/2$ and $\gamma_q^{(2)} = \cos q_x \cos q_y$. $C_{n,m}$ denotes the correlation functions. Assuming rotational symmetry, i.e., $\langle S_i^z \rangle = 0$, they read $C_{n,m} = C_{\mathbf{R}} = \langle S_{\mathbf{R}}^- S_0^+ \rangle = 2 \langle S_{\mathbf{R}}^z S_0^z \rangle$ with $\mathbf{R} = n\mathbf{e}_x + m\mathbf{e}_y$. Calculating the second derivative $-\ddot{S}_q^+$, an approximation as indicated in Refs. 24,28–43 is used which implies the decoupling scheme

$$S_i^+ S_j^+ S_k^- = \alpha_{i,k} \langle S_i^+ S_k^- \rangle S_j^+ + \alpha_{j,k} \langle S_j^+ S_k^- \rangle S_i^+, \quad (3)$$

where the quantities $\alpha_{i,k}$ are vertex parameters introduced to improve the decoupling scheme. In the vicinity of J_2^c a spin nematic phase could be present, and the decoupling scheme (3) might be not appropriate. Therefore, we restrict our consideration to sufficiently large values of J_2 , $J_2 > 0.7|J_1|$, where the semi-classical antiferromagnetic collinear stripe GS LRO is present. Since an $\alpha_{i,k}$ is a function of the lattice vector $\mathbf{R}_i - \mathbf{R}_k$ connecting the sites i and k , in what follows we use the same notation as for the correlation functions $C_{n,m}$, i.e. the vertex parameter $\alpha_{n,m}$ belongs to the lattice vector $\mathbf{R} = n\mathbf{e}_x + m\mathbf{e}_y$. We obtain $-\ddot{S}_q^+ = \omega_q^2 S_q^+$ and

$$\chi_q^{+-}(\omega) = -\langle\langle S_q^+; S_{-q}^- \rangle\rangle_\omega = \frac{M_q}{\omega_q^2 - \omega^2}, \quad (4)$$

with

$$\omega_q^2 = 2 \sum_{k,l=(1,2)} J_k J_l \left(1 - \gamma_q^{(k)}\right) \times \left[K_{k,l} + 8\alpha_{1,k-1} C_{1,k-1} \left(1 - \gamma_q^{(l)}\right) \right], \quad (5)$$

where $K_{1,1} = 1 + 2(2\alpha_{1,1}C_{1,1} + \alpha_{2,0}C_{2,0} - 5\alpha_{1,0}C_{1,0})$, $K_{2,2} = 1 + 2(2\alpha_{2,0}C_{2,0} + \alpha_{2,2}C_{2,2} - 5\alpha_{1,1}C_{1,1})$, $K_{1,2} = 4(\alpha_{1,2}C_{1,2} - \alpha_{1,0}C_{1,0})$, and $K_{2,1} = 4(\alpha_{1,0}C_{1,0} + \alpha_{1,2}C_{1,2} - 2\alpha_{1,1}C_{1,1})$. The correlation functions $C_{n,m}$ are calculated using the spectral theorem,²⁵

$$C_{\mathbf{q}} = \langle S_{\mathbf{q}}^+ S_{\mathbf{q}}^- \rangle = \frac{M_{\mathbf{q}}}{2\omega_{\mathbf{q}}} [1 + 2n(\omega_{\mathbf{q}})], \quad (6)$$

where $n(\omega_{\mathbf{q}}) = (e^{\omega_{\mathbf{q}}/T} - 1)^{-1}$ is the Bose function. Magnetic LRO is reflected by a non-vanishing condensation term C (see, e.g., Refs. 29,34,36) according to $C_{\mathbf{R}} = \frac{1}{N} \sum_{\mathbf{q} \neq \mathbf{Q}} C_{\mathbf{q}} e^{i\mathbf{q}\mathbf{R}} + C e^{i\mathbf{Q}\mathbf{R}}$ where \mathbf{Q} denotes the magnetic ordering vector. The magnetic order parameter (sublattice magnetization) is calculated as

$$m^2 = \frac{3}{2} \frac{1}{N} \sum_{\mathbf{R}} C_{\mathbf{R}} e^{-i\mathbf{Q}\mathbf{R}} = \frac{3}{2} C. \quad (7)$$

The corresponding static susceptibility is given by $\chi_{\mathbf{Q}} = \frac{1}{2} \lim_{\mathbf{q} \rightarrow \mathbf{Q}} \chi_{\mathbf{q}}^{+-}(\omega = 0)$. The uniform static susceptibility is $\chi_0 = \frac{1}{2} \chi_{\mathbf{q}=\mathbf{0}}^{+-}(\omega = 0)$. The correlation length is obtained by an expansion of the static susceptibility around the magnetic ordering vector \mathbf{Q} , $\chi_{\mathbf{Q}+\mathbf{q}}^{+-} \approx \chi_{\mathbf{Q}}^{+-} (1 - \xi_x^2 q_x^2 - \xi_y^2 q_y^2)$, see, e.g., Refs. 24,29,30,36,40. From the on-site correlator $\langle S_i^- S_i^+ \rangle$ and the operator identity $S_i^- S_i^+ = \frac{1}{2} + S_i^z$ we get the sum rule

$$C_0 = \frac{1}{N} \sum_{\mathbf{q}} C_{\mathbf{q}} = \frac{1}{2}. \quad (8)$$

Considering the collinear stripe phase we have two equivalent magnetic ordering vectors, $\mathbf{Q}_1 = (0, \pi)$ and $\mathbf{Q}_2 = (\pi, 0)$. To preserve square-lattice symmetry we follow Ref. 29 and calculate the correlation functions as $C_{n,m} = (C_{n,m}^{(1)} + C_{n,m}^{(2)})/2$ with $C_{n,m}^{(i)} = \frac{1}{N} \sum_{\mathbf{q} \neq \mathbf{Q}_i} C_{\mathbf{q}} e^{i\mathbf{q}\mathbf{R}} + C e^{i\mathbf{Q}_i\mathbf{R}}$. Note that C is the same for \mathbf{Q}_1 and \mathbf{Q}_2 . Analogously, we consider $\chi_{\mathbf{Q}+\mathbf{q}} = (\chi_{\mathbf{Q}_1+\mathbf{q}} + \chi_{\mathbf{Q}_2+\mathbf{q}})/2$ to get the correlation length by expansion of $\chi_{\mathbf{Q}+\mathbf{q}}$ for small \mathbf{q} yielding

$$\xi^2 = \frac{2J_2 C_{1,1}}{4J_1 C_{1,0} + 8J_2 C_{1,1}} + \frac{A}{\Delta}, \quad (9)$$

where $\Delta = 2J_1^2 K_{1,1} + 4J_2^2 K_{2,2} + 2J_1 J_2 (K_{1,2} + 2K_{2,1}) + 16(J_1 + 2J_2)(J_1 \alpha_{1,0} C_{1,0} + 2J_2 \alpha_{1,1} C_{1,1})$ and $A = -J_2^2 (32\alpha_{1,1} C_{1,1} + K_{2,2}) - 4J_1 J_2 (3\alpha_{1,0} C_{1,0} + \alpha_{1,2} C_{1,2})$.

In the GS, LRO may exist, that is, $C \neq 0$. C is determined by^{34,37,41} $\chi_{\mathbf{Q}_1}^{-1} = \chi_{\mathbf{Q}_2}^{-1} = 0$ with

$$\chi_{\mathbf{Q}_i} = -\frac{-4J_1 C_{1,0} - 8J_2 C_{1,1}}{\Delta}. \quad (10)$$

Next we have to discuss the choice of the vertex parameters $\alpha_{n,m}$. Obviously, there are five different $\alpha_{n,m}$ in Eq. (5) which have to be determined together with the corresponding correlation functions $C_{n,m}$. In addition, at zero temperature the condensation term C (describing magnetic LRO) has to be considered. To determine these quantities we can use the Fourier transformation of Eq. (6) providing five equations for $C_{n,m}$. Moreover, at zero temperature we use $\chi_{\mathbf{Q}_1}^{-1} = \chi_{\mathbf{Q}_2}^{-1} = 0$ to calculate C , see above. Finally, only one equation, namely the sum rule (8), is left to find the vertex parameters. Hence, we have to introduce further approximations. In the case of a ferromagnetic GS ($J_2 < J_2^c$) all correlation functions behave quite similar and a reasonable approximation is

to set $\alpha_{n,m} = \alpha$, see, e.g., Refs. 30,34 and 24. This simple approximation was also used in Ref. 33 applying the RGM to antiferromagnets. However, in the antiferromagnetic regime the correlation functions carry different signs, and setting $\alpha_{n,m} = \alpha$ leads to poor results at low temperatures. A significant improvement of the RGM results for antiferromagnets can be achieved by introducing two independent vertex parameters.^{29,34,41} This requires, however, an additional external input to get one more equation. To take into account the dominant character of J_2 in the collinear stripe phase, we set $\alpha_{1,1} = \alpha_1$ and $\alpha_{n,m} = \alpha_2$, $(n,m) \neq (1,1)$. Since the low-temperature properties of the model are related to excitations above the GS, a realistic description of the GS is necessary. Therefore, in the present paper we use, as an additional external input, the GS sublattice magnetization calculated by the CCM.⁴ Thus, describing GS magnetic ordering properly, we may expect that the RGM provides also a reasonable description of the low-temperature properties of the model. This input yields the required additional equation to determine the two independent vertex parameters α_1 and α_2 at $T = 0$. As a result we can also calculate the uniform static susceptibility χ_0 at $T = 0$, cf. Fig. 1.

For finite temperatures we need a reasonable ansatz for the temperature dependence of the ratio α_2/α_1 of the vertex parameters, see, e.g. Refs. 29,34,36 and 42. We have tested several ansatzes to get a proper description of thermodynamic quantities in the whole temperature range, see below. To solve the system of RGM equations we use Broyden's method,⁴⁴ which yields the solutions with a relative error of about 10^{-8} on the average. The momentum integrals are done by Gaussian integration. To find the numerical solution of the equations for $T > 0$, we start at high temperatures and decrease T in small steps. Below a certain (low) temperature $T_0(J_2)$ no solutions of the RGM equations (except at $T = 0$) could be found, since the quantity $\Delta(T, J_2)$ in Eqs. (9) and (10) becomes exponentially small which leads to numerical instabilities. As expected, at large temperatures the concrete choice of the ratio $\frac{\alpha_2}{\alpha_1}(T)$ becomes irrelevant, and even the simple approximation $\alpha_{n,m} = \alpha$ yields results for $\chi_0(T)$ which coincide with the data from the high-temperature expansion. At low temperatures a reasonable ansatz for the ratio α_2/α_1 should (i) provide numerical data down to sufficiently low temperatures and (ii) yield coincidence of $\chi_0(T = 0)$ determined by using the CCM input and $\lim_{T \rightarrow 0} \chi_0(T)$ calculated with the ansatz for $\frac{\alpha_2}{\alpha_1}(T)$. The simplest way is to fix the ratio $\frac{\alpha_2}{\alpha_1}$ to its value at $T = 0$. Tracing the RGM solution to very low temperatures we find that the ansatz

$$\frac{\alpha_2(T)}{\alpha_1(T)} = 1 + \left(\frac{\alpha_2(0)}{\alpha_1(0)} - 1 \right) e^{-\gamma T}, \quad \gamma \geq 0 \quad (11)$$

with the tiny exponent $\gamma = 0.005$ is more appropriate to get numerically stable solutions at low T . Note, however, that our results are not noticeably influenced by the choice of γ , see also Fig. 1. In what follows we use

this ansatz to solve the RGM equations with two vertex parameters.

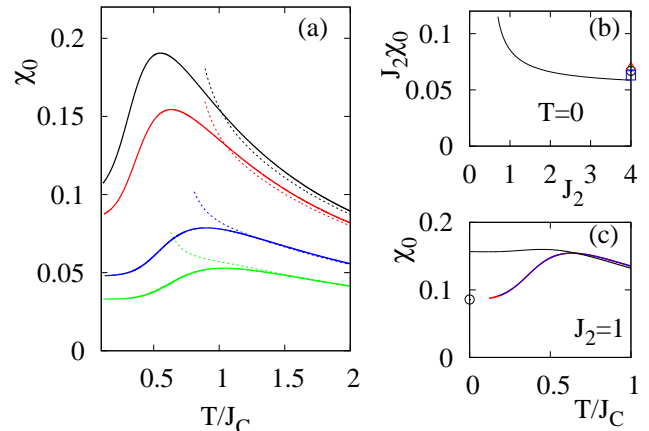


FIG. 1: Uniform susceptibility χ_0 of the J_1 - J_2 model for ferromagnetic $J_1 = -1$.

(a) Temperature dependence of the uniform susceptibility χ_0 for $J_2 = 0.9$ (black), $J_2 = 1.0$ (red), $J_2 = 1.5$ (blue), and $J_2 = 2.0$ (green) calculated by RGM (solid lines). The temperature T is scaled by $J_C = \sqrt{J_1^2 + J_2^2}$. For comparison, eighth-order high-temperature expansion results (Refs. 19,20) are shown (dashed lines).

(b) Ground-state values for $J_2\chi_0$ vs. J_2 . The susceptibility data for the square-lattice antiferromagnet (quantum Monte Carlo⁴⁵ - black circle, CCM⁴⁷ - red triangle, third-order spin-wave theory⁴⁶ - blue square) are also shown as data points at $J_2 = 4$.

(c) Comparison of the temperature dependence of the uniform susceptibility χ_0 for $J_2 = 1$ calculated using three different choices of the vertex parameters (red line - two vertex parameters with the ansatz (11) and $\gamma = 0.005$, blue line - two vertex parameters with fixed ratio $\frac{\alpha_2}{\alpha_1}(T) = \frac{\alpha_2}{\alpha_1}(0)$ (i.e. ansatz (11) with $\gamma = 0$), black line - only one vertex parameter). Note that the red and the blue lines practically coincide. Note further that the red line extends down to slightly lower temperatures. The black circle at $T = 0$ shows the zero-temperature RGM value for χ_0 calculated with two vertex parameters.

III. RESULTS AND DISCUSSION

In what follows we fix the ferromagnetic NN exchange to $J_1 = -1$. We focus on sufficiently large values of J_2 , $J_2 > 0.7$, where a possible nematic GS phase is not present, and, rather the GS exhibits semi-classical collinear magnetic LRO. Moreover, the experimental data for layered oxovanadates^{8,9,15} correspond to this parameter regime. We follow Ref. 21 and use as a characteristic energy scale $J_C = \sqrt{J_1^2 + J_2^2}$, see also Refs. 9,15.

In Fig. 1(a) the temperature dependence of the uniform susceptibility χ_0 is shown. For comparison we also

present the results of the eighth order high-temperature expansion,²⁰ which agree with the RGM data at large T . In Fig. 1(b) the GS results for the susceptibility $\chi_0(T=0)$ are presented. Since for large J_2 the J_1 - J_2 model corresponds to a system of two inter-penetrating square-lattice antiferromagnets with coupling strength J_2 , our RGM data for $\chi_0(T=0)$ can be compared with available GS results for $\chi_0(T=0)$ of the square-lattice antiferromagnet,^{45–47} see data points at $J_2=4$ in Fig. 1(b). For large J_2 , the dependence of $J_2\chi_0(T=0)$ on J_2 is weak down to $J_2 \sim 1$. A noticeable upturn of $J_2\chi_0(T=0)$ for small J_2 may indicate the approach to the ferromagnetic phase. In Fig. 1(c) we compare different choices of the vertex parameters to solve the RGM equations, see the discussion in Sec. II. Obviously, the use of only one vertex parameter by setting $\alpha_{n,m} = \alpha$ leads to poor results for $T \lesssim 0.6J_C$. On the other hand, the two choices of the parameter γ in the ansatz (11) lead to almost identical $\chi_0(T)$ curves.

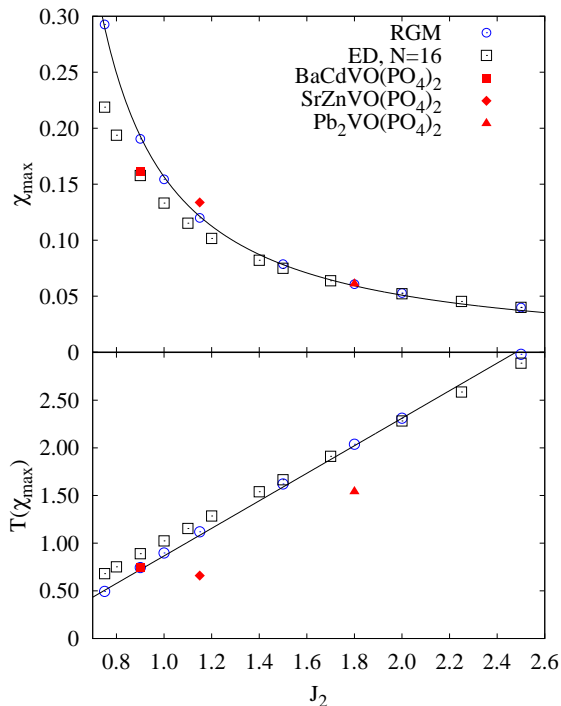


FIG. 2: Height and position of the maximum of the susceptibility $\chi_0(T)$ for the J_1 - J_2 model with $J_1 = -1$ in dependence on the frustration parameter J_2 . The blue circles are the RGM results, the open squares show the ED data for $N = 16$, the lines correspond to Eqs. (12) and (13), and the colored filled symbols correspond to $\text{BaCdVO}(\text{PO}_4)_2$ ($J_2/|J_1| \approx 0.9$)⁹, $\text{SrZnVO}(\text{PO}_4)_2$ ($J_2/|J_1| \approx 1.15$)¹⁵, and $\text{Pb}_2\text{VO}(\text{PO}_4)_2$ ($J_2/|J_1| \approx 1.8$)⁸.

For the comparison with experimental data on oxovanadate compounds, such as $\text{BaCdVO}(\text{PO}_4)_2$, $\text{SrZnVO}(\text{PO}_4)_2$, and $\text{Pb}_2\text{VO}(\text{PO}_4)_2$ ^{8,9,15}, the height

χ_{max} and the position $T(\chi_{max})$ of the maximum in the $\chi_0(T)$ curve are interesting features. However, in these compounds, due to a weak interlayer coupling, a phase transition to magnetic long-range order at a critical temperature T_N was detected,^{8,9,15} where $T_N/|J_1| \sim 0.28, 0.35$, and 0.48 was found for $\text{BaCdVO}(\text{PO}_4)_2$, $\text{SrZnVO}(\text{PO}_4)_2$, and $\text{Pb}_2\text{VO}(\text{PO}_4)_2$, respectively. Since in our paper we deal with a strictly two-dimensional model, such a comparison is reasonable only in the paramagnetic phase of the compounds, i.e. at $T > T_N$, where two-dimensional spin physics dominates the thermodynamic behavior. Indeed, the relevant temperatures $T(\chi_{max})$ are well above T_N for all three oxovanadates, namely $T(\chi_{max})/|J_1| = 0.75, 0.66$, and 1.54 for $\text{BaCdVO}(\text{PO}_4)_2$, $\text{SrZnVO}(\text{PO}_4)_2$, and $\text{Pb}_2\text{VO}(\text{PO}_4)_2$, respectively, see Fig. 2.

We mention, that χ_{max} and $T(\chi_{max})$ have been presented as functions of $\tan^{-1}(J_2/J_1)$ for the whole parameter space of J_1 and J_2 in Ref. 21 using full ED for $N = 8, 16$ and 20 sites, see Fig. 17 in Ref. 21. We have recalculated the corresponding ED data for $N = 16$. In Fig. 2 we show the ED and the RGM results for χ_{max} and $T(\chi_{max})$ as functions of J_2 in the parameter region $J_2 > 0.7$ considered in our paper.

The RGM data points are well described by the relations

$$\chi_{max} = a(J_2 - J_2^c)^{-\nu}, \quad (12)$$

$$T(\chi_{max}) = b(J_2 - J_2^c) \quad (13)$$

with $a = 0.0872$, $\nu = 1.146$, $b = 1.444$, and $J_2^c = 0.4$. Note, however, that the divergence of χ_{max} at $J_2^c = 0.4$ suggested by Eq. (12) might be absent in the considered model, since our approach is not designed for $J_2 \sim J_2^c$. Using experimental data of the susceptibility for quasi-two-dimensional frustrated square-lattice magnets as well as the reported exchange constants J_1 and J_2 we can compare our theoretical data directly with experiment, see Fig. 2. Obviously, theory and experiment agree well, particularly for χ_{max} . Hence, our equations (12) and (13) can be used to get information on the ratio $J_2/|J_1|$ from susceptibility measurements.

Next we discuss the correlation length ξ . Its temperature dependence is depicted in Fig. 3 for different values of the frustration parameter J_2 . With increasing NNN exchange J_2 the rapid increase in ξ is shifted to larger temperatures. As shown in the inset of Fig. 3, at a certain fixed temperature, ξ decreases rapidly with decreasing J_2 .

The exponential low-temperature divergence of $\xi \propto e^{A/T}$ for two-dimensional Heisenberg magnets with NN interactions is determined by the spin stiffness ρ_s , i.e. $A \propto \rho_s$, see e.g. Refs. 24,49–53. As it has been recently reported,²⁴ for small J_2 , where a ferromagnetic GS is present, the relation $\xi \propto e^{a\rho_s/T}$ also holds if the NNN exchange J_2 is included. In this case the stiffness was obtained from the RGM dispersion relation²⁴ as $\rho_s^{FM} = -(J_1 + 2J_2)/4$. For the antiferromagnetic collinear stripe GS phase present at large J_2 one may

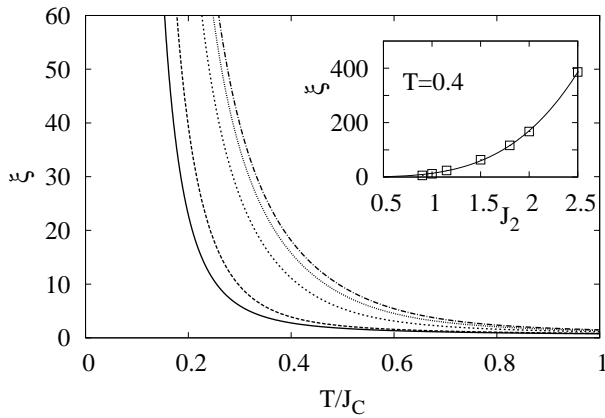


FIG. 3: Temperature dependence of the correlation length ξ (in units of the lattice spacing) for different values of the frustration parameter $J_2=0.9, 1.0, 1.5, 2.0$ and 2.5 (from left to right). The temperature T is scaled by $J_C = \sqrt{J_1^2 + J_2^2}$. The inset shows the correlation length for $T = 0.4$ in dependence on the frustration parameter J_2 . The solid line represents a fit to the data points (open squares).

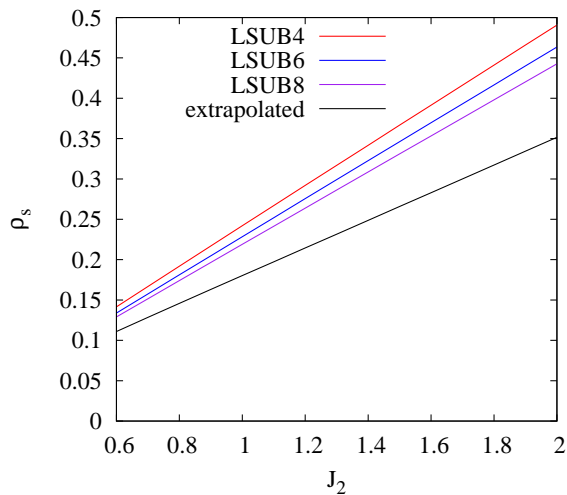


FIG. 4: Spin stiffness ρ_s of the J_1 - J_2 model for ferromagnetic $J_1 = -1$ as a function of J_2 calculated by the CCM.

expect that the stiffness also determines the exponential divergence at small T . However, the determination of ρ_s is more difficult. Here we use the CCM^{54–56} to provide data for ρ_s . To calculate ρ_s within the CCM we follow strictly Refs. 55 and 56 and do not explain details of the calculation. The stiffness as a function of J_2 is shown in Fig. 4 for various levels of CCM approximations, LSUB n , as well as extrapolated data.⁵⁷ The obvious (almost) linear J_2 -dependence of ρ_s is well described for the extrapolated CCM data by $\rho_s \approx 0.175J_2$. Hence, it seems to be reasonable to show the tempera-

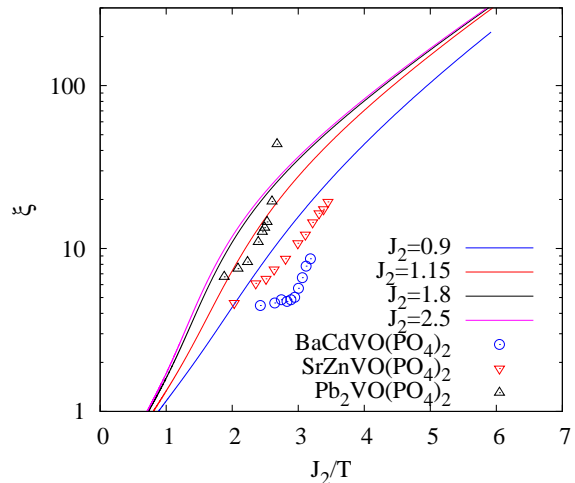


FIG. 5: Correlation length ξ (logarithmic scale) in units of the lattice spacing vs. J_2/T calculated using RGM (lines) for various values of the frustration parameter J_2 . For comparison we also show experimental data¹⁵ for $\text{BaCdVO}(\text{PO}_4)_2$ ($J_2/|J_1| \approx 0.9$), $\text{SrZnVO}(\text{PO}_4)_2$ ($J_2/|J_1| \approx 1.15$), and $\text{Pb}_2\text{VO}(\text{PO}_4)_2$ ($J_2/|J_1| \approx 1.8$).

ture dependence of the correlation length, in addition to Fig. 3, as a function $\ln \xi(J_2/T)$, see Fig. 5. First we notice that the experimental data reported in Ref. 15 agree reasonably well with our RGM results. Secondly, it is obvious that for large values of $J_2 \gtrsim 1.5$ the $\ln \xi(J_2/T)$ curves almost coincide. The small deviations can be attributed to a temperature dependent prefactor in front of the exponential term.^{24,49–53} However, for $J_2 = 1.15$ and $J_2 = 0.9$ the theoretical as well as the experimental data show deviations from the behavior suggested by the stiffness data.

IV. SUMMARY

Using second-order Greens function technique we have calculated the uniform susceptibility χ_0 and the correlation length ξ of the frustrated J_1 - J_2 square-lattice Heisenberg ferromagnet in the collinear antiferromagnetic regime present for large values of $J_2/|J_1|$. We have derived simple power laws for the height and the position of the maximum in the $\chi_0(T)$ curve as functions of J_2 . We have found that our theoretical data agree reasonably well with recent experiments on oxovanadates.

Acknowledgment The authors are indebted to O. Derzhko for critical reading of the manuscript. J.R. and S.-L.D. thank the DFG for financial support (grants DR269/3-3 and RI615/16-3).

- ¹ H. J. Schulz and T. A. L. Ziman, *Europhys. Lett.* **18**, 355 (1992); H. J. Schulz, T. A. L. Ziman, and D. Poilblanc, *J. Phys. I* **6**, 675 (1996).
- ² N. Shannon, T. Momoi, and P. Sindzingre, *Phys. Rev. Lett.* **96**, 027213 (2006).
- ³ J. Richter and J. Schulenburg, *Eur. Phys. J. B* **73**, 117 (2010).
- ⁴ J. Richter, R. Darradi, J. Schulenburg, D. J. J. Farnell, and H. Rosner, *Phys. Rev. B* **81**, 174429 (2010).
- ⁵ H. Feldner, D. C. Cabra, and G. L. Rossini, *Phys. Rev. B* **84**, 214406 (2011).
- ⁶ J. Reuther and P. Wölfle, *Phys. Rev. B* **81**, 144410 (2010).
- ⁷ Ling Wang, Zheng-Cheng Gu, Xiao-Gang Wen, and F. Verstraete, arXiv:1112.3331
- ⁸ E. E. Kaul, H. Rosner, N. Shannon, R.V. Shpanchenko, and C. Geibel, *J. Magn. Magn. Mater.* **272-276(II)**, 922 (2004).
- ⁹ R. Nath, A.A. Tsirlin, H. Rosner, and C. Geibel, *Phys. Rev. B* **78**, 064422 (2008).
- ¹⁰ P. Carretta, M. Filibian, R. Nath, C. Geibel, and P. J. C. King, *Phys. Rev. B* **79**, 224432 (2009).
- ¹¹ M. Skoulatos, J.P. Goff, C. Geibel, E.E. Kaul, R. Nath, N. Shannon, B. Schmidt, A.P. Murani, P.P. Deen, M. Enderle, and A.R. Wildes, *Europhys. Lett.* **88**, 57005 (2009).
- ¹² R. Nath, Y. Furukawa, F. Borsa, E. E. Kaul, M. Baenitz, C. Geibel, and D. C. Johnston, *Phys. Rev. B* **80**, 214430 (2009).
- ¹³ A.A. Tsirlin and H. Rosner, *Phys. Rev. B* **79**, 214417 (2009).
- ¹⁴ A.A. Tsirlin, B. Schmidt, Y. Skourski, R. Nath, C. Geibel, and H. Rosner, *Phys. Rev. B* **80**, 132407 (2009).
- ¹⁵ L. Bossoni, P. Carretta, R. Nath, M. Moscardini, M. Baenitz, and C. Geibel, *Phys. Rev. B* **83**, 014412 (2011).
- ¹⁶ A. A. Tsirlin, R. Nath, A. M. Abakumov, Y. Furukawa, D. C. Johnston, M. Hemmida, H.-A. Krug von Nidda, A. Loidl, C. Geibel, and H. Rosner, *Phys. Rev. B* **84**, 014429 (2011).
- ¹⁷ D. C. Johnston, R. J. McQueeney, B. Lake, A. Honecker, M. E. Zhitomirsky, R. Nath, Y. Furukawa, V. P. Antropov, and Y. Singh, *Phys. Rev. B* **84**, 094445 (2011).
- ¹⁸ M. Troyer and U.-J. Wiese, *Phys. Rev. Lett.* **94**, 170201 (2005).
- ¹⁹ H. Rosner, R.R.P. Singh, W.H. Zheng, J. Oitmaa, and W.E. Pickett, *Phys. Rev. B*, **67**, 014416 (2003).
- ²⁰ H.-J. Schmidt, A. Lohmann, and J. Richter, *Phys. Rev. B* **84**, 104443 (2011).
- ²¹ N. Shannon, B. Schmidt, K. Penc, P. Thalmeier, *Eur. Phys. J. B* **38**, 599 (2004).
- ²² B. Schmidt, N. Shannon, and P. Thalmeier, *J. Phys. Cond. Mat.* **19**, 145211 (2007).
- ²³ B. Schmidt, N. Shannon, and P. Thalmeier, *J. Magn. Magn. Mater.* **310**, 1231 (2007).
- ²⁴ M. Härtel, J. Richter, D. Ihle, and S.-L. Drechsler, *Phys. Rev. B* **81**, 174421 (2010).
- ²⁵ W. Gasser, E. Heiner, and K. Elk, *Greensche Funktionen in Festkörper- und Vielteilchenphysik* (Wiley, Berlin 2001).
- ²⁶ P. Froebrich and P.J. Kuntz, *Physics Reports* **432**, 223 (2006).
- ²⁷ Yu. G. Rudoy, *Theor. Math. Phys.* **168**, 1318 (2011).
- ²⁸ A.F. Barabanov and V.M. Berezovskii, *J. Phys. Soc. Jpn.* **63**, 3974 (1994); *Phys. Lett. A* **186**, 175 (1994); *Zh. Eksp. Teor. Fiz.* **106**, 1156 (1994) [*JETP* **79**, 627 (1994)].
- ²⁹ L. Siurakshina, D. Ihle, and R. Hayn, *Phys. Rev. B* **64**, 104406 (2001).
- ³⁰ M. Härtel, J. Richter, D. Ihle, and S.-L. Drechsler, *Phys. Rev. B* **78**, 174412 (2008); J. Richter, M. Härtel, D. Ihle, and S.-L. Drechsler, *J.Phys.:Conf.Ser.* **145**, 012064 (2009); M. Härtel, J. Richter, D. Ihle, J. Schnack, and S.-L. Drechsler, *Phys. Rev. B* **84**, 104411 (2011).
- ³¹ A.V. Mikheenkov, N.A. Kozlov, and A.F. Barabanov, *Physics Letters A* **373**, 693 (2009).
- ³² A. F. Barabanov, A. V. Mikheenkov, and A. V. Shvartsberg, *Theor. Math. Phys.* **168**, 1192 (2011).
- ³³ J. Kondo and K. Yamaji, *Prog. Theor. Phys.* **47**, 807 (1972).
- ³⁴ H. Shimahara and S. Takada, *J. Phys. Soc. Jpn.* **60**, 2394 (1991).
- ³⁵ F. Suzuki, N. Shibata, and C. Ishii, *J. Phys. Soc. Jpn.* **63**, 1539 (1994).
- ³⁶ S. Winterfeldt and D. Ihle, *Phys. Rev. B* **56**, 5535 (1997).
- ³⁷ D. Ihle, C. Schindelin, A. Weiße, and H. Fehske, *Phys. Rev. B* **60**, 9240 (1999).
- ³⁸ W. Yu and S. Feng, *Eur. Phys. J. B* **13**, 265 (2000).
- ³⁹ B.H. Bernhard, B. Canals, and C. Lacroix, *Phys. Rev. B* **66**, 104424 (2002).
- ⁴⁰ D. Schmalfuß, J. Richter, and D. Ihle, *Phys. Rev. B* **70**, 184412 (2004); D. Schmalfuß, J. Richter, and D. Ihle, *Phys. Rev. B* **72**, 224405 (2005).
- ⁴¹ D. Schmalfuß, R. Darradi, J. Richter, J. Schulenburg, and D. Ihle, *Phys. Rev. Lett.* **97**, 157201 (2006).
- ⁴² I. Juhász Junger, D. Ihle, and J. Richter, *Phys. Rev. B* **80**, 064425 (2009).
- ⁴³ I. Juhász Junger, D. Ihle, L. Bogacz, and W. Janke *Phys. Rev. B* **77**, 174411 (2008).
- ⁴⁴ W.H. Press, S.A. Teukolsky, W.T. Vetterling, B.P. Flannery, *Numerical Recipes in C++, The Art of Scientific Computing* (Cambridge University Press, Cambridge, 2007).
- ⁴⁵ K.J. Runge, *Phys. Rev. B* **45**, 12292 (1992).
- ⁴⁶ C.J. Hamer, Zheng Weihong, and P. Arndt, *Phys. Rev. B* **46**, 6276 (1992).
- ⁴⁷ D. J. J. Farnell, R. Zinke, J. Schulenburg, and J. Richter, *J. Phys.: Condens. Matter* **21**, 406002 (2009).
- ⁴⁸ M. Takahashi, *Prog. Theo. Phys. Supp.* **87**, 233 (1986); M. Takahashi, *Phys. Rev. Lett.* **58** 168 (1987).
- ⁴⁹ A. Auerbach and D. Arovas, *Phys. Rev. Lett.* **61**, 617 (1988).
- ⁵⁰ S. Chakravarty, B. I. Halperin, and D. R. Nelson, *Phys. Rev. B* **39**, 2344 (1989).
- ⁵¹ P. Kopietz and S. Chakravarty, *Phys. Rev. B* **40**, 4858 (1989).
- ⁵² P. Hasenfratz and P. Niedermayer, *Phys. Lett. B* **268**, 231 (1991).
- ⁵³ M. Greven, R. J. Birgeneau, Y. Endoh, M. A. Kastner, B. Keimer, M. Matsuda, G. Shirane, and T. R. Thurston, *Phys. Rev. Lett.* **72**, 1096 (1994).
- ⁵⁴ D. J. J. Farnell and R. F. Bishop, in *Quantum Magnetism*, Lecture Notes in Physics Vol. **645**, edited by U. Schollwöck, J. Richter, D. J. J. Farnell, and R. F. Bishop (Springer, Berlin, 2004), p. 307.
- ⁵⁵ S.E. Krüger, R. Darradi, J. Richter, and D.J.J. Farnell, *Phys. Rev. B* **73**, 094404 (2006).

- ⁵⁶ R. Darradi, O. Derzhko, R. Zinke, J. Schulenburg, S. E. Krüger, and J. Richter, Phys. Rev. B **78**, 214415 (2008).
- ⁵⁷ The LSUB n approximation scheme is widely used in CCM calculations, see e.g. Refs.54–56. Within the LSUB n scheme all multispin correlations over all distinct locales on

the lattice defined by n or fewer contiguous sites are taken into account. Since the LSUB n approximation becomes exact for $n \rightarrow \infty$, it is useful to extrapolate the "raw" LSUB n data to $n \rightarrow \infty$ by $\rho_s(n) = c_0 + c_1(1/n) + c_2(1/n)^2$.